We are IntechOpen, the world's leading publisher of Open Access books Built by scientists, for scientists

6,900
Open access books available

186,000
International authors and editors

200M
Downloads

Our authors are among the

154
Countries delivered to

TOP 1%
most cited scientists

12.2%
Contributors from top 500 universities

BOOK CITATION INDEX
CLARIVATE ANALYTICS
INDEXED

WEB OF SCIENCE™

Selection of our books indexed in the Book Citation Index
in Web of Science™ Core Collection (BKCI)

Interested in publishing with us?
Contact book.department@intechopen.com

Cell Cycle Analysis of ER Stress and Autophagy

Ashik Asvin Patel and Gary Warnes

Additional information is available at the end of the chapter

Abstract

Cell cycle-arresting drugs, thapsigargin (Tg) and chloroquine (CQ), are employed to study endoplasmic reticulum (ER) stress and the autophagic process using cell lines without measuring the cell cycle of such cells. The potential cell cycle-dependent aspect of such processes in cell lines may impact upon the degree of ER stress and autophagy measured. ER stress is known to be caused by a build-up of misfolded proteins within the ER, which may then undergo ER phagy or reticulophagy. The cell cycle-dependent nature of all these processes is not well studied, so we investigated ER stress and autophagy by use of a combination of flow cytometric assays. These included cell cycle-dependent measurement of reticulophagy, misfolded protein levels and autophagic marker LC3-II in K562 and Jurkat cells. ER stress-inducing drug Tg caused significant reticulophagy in both cell types. This was cell cycle dependent in K562 cells only, with proliferating cells undergoing more reticulophagy. In contrast, autophagy-initiating drug CQ caused reticulophagy at higher doses in Jurkat cells, whereas K562 cells showed a cell cycle-dependent elongation of the ER, which was less pronounced in proliferating cells. The level of cellular misfolded protein in response to both drugs was high in K562 cells when either undergoing reticulophagy or elongation in a non-cell cycle-dependent manner, whereas the misfolded protein levels in Jurkat cells in response to both drugs were lower than those observed in K562 cells. Both cell lines employed in this study showed no increase of LC3-II above controls in response to Tg treatment. However, CQ induced a cell cycle-dependent increase of LC3-II in both cell types. Thus, the type of cell employed and the cell cycle dependent modulation of thebiological processes involved in ER stress and autophagy should be considered when designing studies in ER stress and autophagy.

Keywords: reticulophagy, ER stress, misfolded proteins, autophagy, flow cytometry

1. Introduction

Endoplasmic reticulum (ER) stress has been implicated in numerous degenerative neurological diseases and cancer; elucidation of the mechanisms involved may determine drug targets for the treatment of such diseases [1, 2]. ER stress is known to cause autophagy and ultimately cell death via apoptosis, the mechanism of which is only beginning to be understood [3–5]. ER stress can be induced by a range of drugs, including thapsigargin (Tg) which acts by inhibition of ER ATPase located in the ER, resulting in the accumulation of misfolded proteins within the ER [6]. Tg is also known to cause cell arrest in G_1 phase of the cell cycle and has been shown to inhibit autophagic flux by inhibition of the translocation of Rab7, a protein required for the fusion of lysosomes with autophagosomes [6–8]. ER stress resulting from a build-up of misfolded proteins occurs once a threshold of misfolded protein accumulation has been reached. This then initiates the unfolded protein response (UPR) by the ER stress sensor signalling proteins, IRE1, PERK and ATF6 which initiate protein refolding and elongation of the ER until ER homeostasis is returned [3, 9, 10]. This process is a coping mechanism which reduces the mass of misfolded protein per unit volume of ER. If the high level of misfolded protein persists, then reticulophagy (phagy of the ER) occurs [11]. Chloroquine (CQ) is also known to initiate autophagy and block completion of the autophagic process by increasing the pH within the lysosome, with resultant inhibition of the lysosome fusion process with autophagosomes [12]. CQ was investigated for its ER stress-inducing qualities by comparison with Tg upon Jurkat T cells and K562 erythromyeloid cell lines. Thus measurement of changes in ER mass and misfolded protein levels would give a measure of the degree of ER stress within a cell.

The term autophagy or type II cell death is derived from the Greek roots "auto" (self) and "phagy" (eat) and was first observed by Porter in 1962 [13, 14]. Autophagy or macroautophagy is an intracellular degradation system that maintains cell homeostasis and is characterised by the formation of a double membrane around the cytosolic components to be degraded, forming an autophagosome of sequestered malfunctioning components ranging from misfolded proteins to organelles such as stressed ER [15, 16]. An autophagosome then fuses with lysosomes, giving rise to an autolysosome, where the intracellular components are degraded by hydrolases which produces energy, thus promoting cellular haemostasis [2, 15, 17–20]. The main biological autophagy marker is the microtubule-associated protein LC3-II or LC3B. LC3-I is normally located in the cytoplasm but when cleaved and lipidated by phosphatidylethanolamine is then incorporated into the autophagosome inner leaflet of the membrane in the form of LC3-II [21–23].

Methods for monitoring autophagy began with the initial discovery of the process by the use of electron microscopy, which showed the presence of autophagosome and autolysosome or autophagolysosome [13, 14]. Biochemical techniques such as Western blotting can be used to quantitate the degree of autophagy in cells by measuring the autophagy marker proteins, LC3-II and LC3-I [21–23]. Fluorescently tagged LC3-II can also be imaged and flow cytometrically analysed through transfections with GFP-RFP through transfections with GFP-RFP, with the benefit that GFP fluorescence is dissipated by the acidic conditions prevailing in autolyso-

somes, whereas RFP is not, thus making LC3-II-GFP detection specific for autophagosomes and LC3-II-RFP specific for autolysosomes [22, 24–26]. The number and intensity of fluorescently labelled anti-LC3-II-positive puncta (autophagosomes-autolysosomes) can also be quantitated by time-consuming image analysis, whereas measuring the increase in median fluorescent values of LC3-II antigen level flow cytometrically makes the process significantly less burdensome, especially when combined with cell cycle analysis [25, 27–29]. Here we show how flow cytometry can be used to measure not only the autophagy marker LC3-II but also the cellular end products of ER stress which include reticulophagy and cellular levels of misfolded proteins and their cell cycle distribution. Most studies using cell lines have not generally focussed upon the cell cycle distribution of the autophagy marker even though autophagy-inducing drugs such as rapamycin are known to cause G_1 cell cycle arrest. However a few studies have investigated the cell cycle distribution of LC3-II with variable results which seem to vary depending upon the cell line employed [17, 30, 31]. Thus this chapter investigates whether the autophagic biological marker, LC3-II, and end products of ER stress (ER mass and misfolded protein) showed a cell cycle-dependent nature during ER stress. Drugs such as Tg and CQ, which cause the build-up of misfolded proteins and induce ER stress, were then compared in terms of cell cycle-dependent reticulophagy, misfolded protein levels and LC3-II [32].

Here, we employed flow cytometric cell cycle analysis of live cells to measure reticulophagy combined with an assay employing fixed-cell immunofluorescence analysis of LC3-II developed in this laboratory and the cell cycle analysis of cellular misfolded proteins [31, 33, 34]. The use of ER Tracker was used as previously described but was now employed in a cell cycle-dependent manner to determine the relative change in ER mass compared to untreated control cells [35, 36]. We also determined the degree of misfolded protein aggregate formation in a cell cycle-dependent manner using the Proteostat probe (Enzo Life Sciences) that fluoresces when bound to misfolded proteins in fixed cells [32]. Thus, we were able to investigate whether the observed drug-induced ER stress had a cell cycle-dependent nature by the measurement of changes in ER mass, misfolded proteins and the autophagy marker LC3-II.

2. Materials and methods

2.1. Induction of ER stress

Jurkat and K562 cells were grown in RPMI-1640 with L-glutamine with 10% FBS (Invitrogen, UK) and penicillin and streptomycin or treated with CQ at 25, 50 and 75 μM (Sigma Chemicals, UK) or 0.1, 0.5 and 1 μM Tg (Santa Cruz, US) for 24 h (n = 3). Cells were harvested and processed as described in the sections below.

2.2. Cell cycle and ER Tracker

Jurkat and K562 cells with or without treatment were adjusted to 1×10^6/ml and loaded with Hoechst 33342 (15 μg/ml, Sigma Chemicals, UK) and ER Tracker Red dye (ERTR 100 nM, Invitrogen, UK), by incubating cells with the dyes for 1 and 0.5 h at 37°C, respectively. Dead

cells were detected by DRAQ7 (2.5 µM, Biostatus, UK), incubated with cells for 10 min at 37°C. Live cells were analysed for ERTR Area MFI levels from Ho33343 Area and Width dot plots; see **Figure 1**. The percentage change in ER mass test samples was determined by comparing test and control values for each phase of the cell cycle comparing control values for each phase of the cell cycle: 30,000 events collected by flow cytometry, with Ho33342 excited at 350–60 nm (UV laser) and emission collected at 450/50 nm; ERTR Area excited at 488 nm (blue laser) and emission collected at 610/10 nm; and DRAQ7 excited at 633 nm (red laser) and emission collected at 780/60 nm (n = 3).

2.3. Misfolded protein labelling

Jurkat and K562 cells with or without treatment were pelleted and resuspended in 200 µl of Solution A fixative for 15 min at room temperature (RT) (Caltag, UK). Cells were then
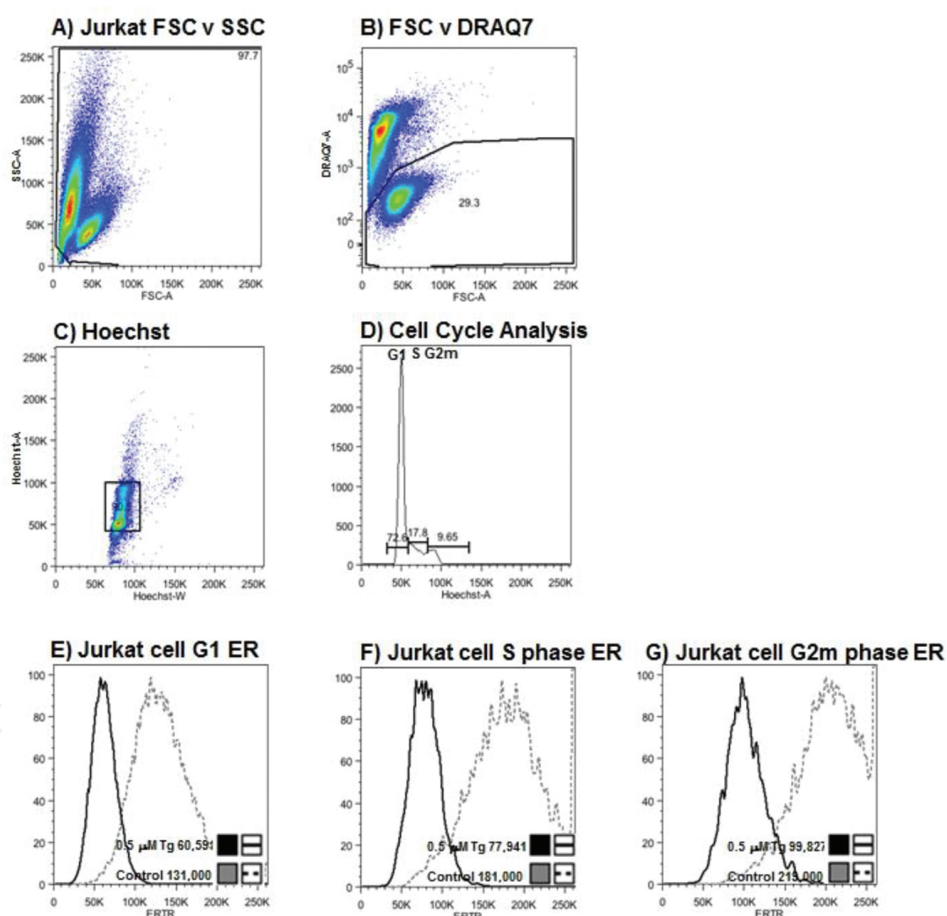

Figure 1. Cells were gated on forward-scatter (FSC) vs. side-scatter (SSC) dot plot (A). Live cells were then gated by their exclusion of cell viability dye DRAQ7 from a FSC vs. DRAQ7 dot plot (B). Live single cells were then gated through Ho33342 Area and Width parameter analysis (C). Cell cycle analysis of these single cells into G_1, S and G_2m phases of the cell cycle by virtue that Ho33342 fluorescence intensity being proportional to DNA content as shown in (D). The ERTR fluorescence signal is proportional to ER mass; the phases of the cell cycle in cells treated with Tg were compared to untreated cells in G_1 (E), S phase (F) and G_2m (G). ERTR MFI were normalised as a percentage change in the test ERTR signal was made to the control ERTR signal.

washed in PBS buffer (Invitrogen, UK) and cell pellets permeabilised with 0.25% Triton X-100 (Sigma Chemicals, UK) for 15 min at RT. Cells were then washed in PBS buffer and a 1:20,000 dilution of Proteostat (Enzo Life Sciences, UK) was made in Proteostat buffer (1 µl of Proteostat reagent in 20 ml of buffer) and 400 µl added to the cell pellet with 1 µg/ml DAPI and incubated for 30 min at RT. Flow cytometric analysis was performed with excitation of Proteostat with the blue 488 nm laser and excitation of DAPI with UV laser line and emissions collected at 610/20 nm and 440/40 nm, respectively (n = 3). Cell cycle analysis was performed by collecting 30,000 events with the DAPI 440/40 Area and Width parameter for doublet discrimination; see **Figure 3**. Then Proteostat Area MFI for cells in G_1, S phase and G_2m cycling cells was determined by comparison of control and test MFI for each phase of the cell cycle by the formula given in the manufacturer's instructions, $(MFI_{test} − MFI_{con})/MFI_{test} × 100$ = misfolded protein level.

2.4. Indirect immunofluorescence LC3-II labelling and cell cycle analysis

Jurkat and K562 cells with or without treatment were pelleted and resuspended in 200 µl of Solution A fixative for 15 min at RT (Caltag, UK). Cells were then washed in PBS buffer and cell pellets permeabilised with 0.25% Triton X-100 for 15 min at RT. Cells were washed in PBS and anti-LC3-II monoclonal antibody (1:400 dilution) (Cat. No. 3868, Cell Signalling Technology Inc., USA) incubated for 0.5 h at RT. Cells were then washed in PBS and labelled with 0.125 µg of secondary fluorescent conjugate Alexa Fluor-647 goat anti-rabbit IgG (Invitrogen, UK) for 0.5 h at RT. Cells were then washed in PBS buffer and resuspended in 400 µl of PBS with DAPI (1 µg/ml). Analysis of upregulated LC3-II-Alexa Fluor-647 MFI signal in treated samples (above control levels) was determined for each phase of the cell cycle by gating cells on a FSC versus SSC dot plot, with doublet discrimination achieved by use of the DAPI Area and Width parameters with gating for G_1, S and G_2m on the DAPI-A parameter; see **Figure 5**. Thirty thousand events were collected by flow cytometry. DAPI was excited at 350–60 nm (UV laser) and emission collected at 450/50 nm; LC3-II-AF-647 was excited at 633 nm (red laser) and emission collected at 660/20 nm (n = 3).

2.5. Flow cytometry

A Becton Dickinson LSRII with FACSDiva software (ver 6.3.1) fitted with blue (488 nm), red (633 nm), violet (405 nm) and UV (350–360 nm) lasers. The optical filters (fitted in 2005) used were for ERTR (610/10 nm), Ho33342 and DAPI (450/50 nm), DRAQ7 (780/60 nm), LC3B-AF-647 (660/20 nm) and Proteostat (610/10 nm).

2.6. Statistics

Student t tests were performed in GraphPad software with $P > 0.05$ not significant (NS), $P < 0.05$*, $P < 0.01$**, n = 3.

3. Results

3.1. Flow cytometric analysis of cell cycle-dependent reticulophagy

For estimating the degree of reticulophagy after treatment with Tg or CQ, known ER stress inducers and interceptor of autophagy, cells were labelled with Ho33342, ERTR and DRAQ7. Live cells were analysed for reticulophagy after flow cytometric analysis on a Becton Dickinson LSRII after UV, blue and red laser excitation and fluorescence collection at 460, 610 and 780 nm, respectively. The gating strategy for the analysis of live cell cycle-dependent reticulophagy of such cells is shown in **Figure 1**.

Tg induced a high degree of K562 cell cycle-dependent reticulophagy (29–76%), which was greater in S, G_2m and G_1 phases with increasing [Tg] ($P < 0.05$, 0.01, n = 3, **Figure 2A**), whereas Jurkat cells displayed a lower level of reticulophagy 35 to >55%, which was not cell cycle dependent ($P < 0.01$, n = 3, **Figure 2B**). The K562 response to CQ was very different to that of Tg with an ER elongation of >10 to >40%, with the highest degree of ER stress (smallest amount of elongation) present in G_2m cells (NS, $P < 0.05$, <0.01, n = 3, **Figure 2C**). CQ treatment of Jurkat
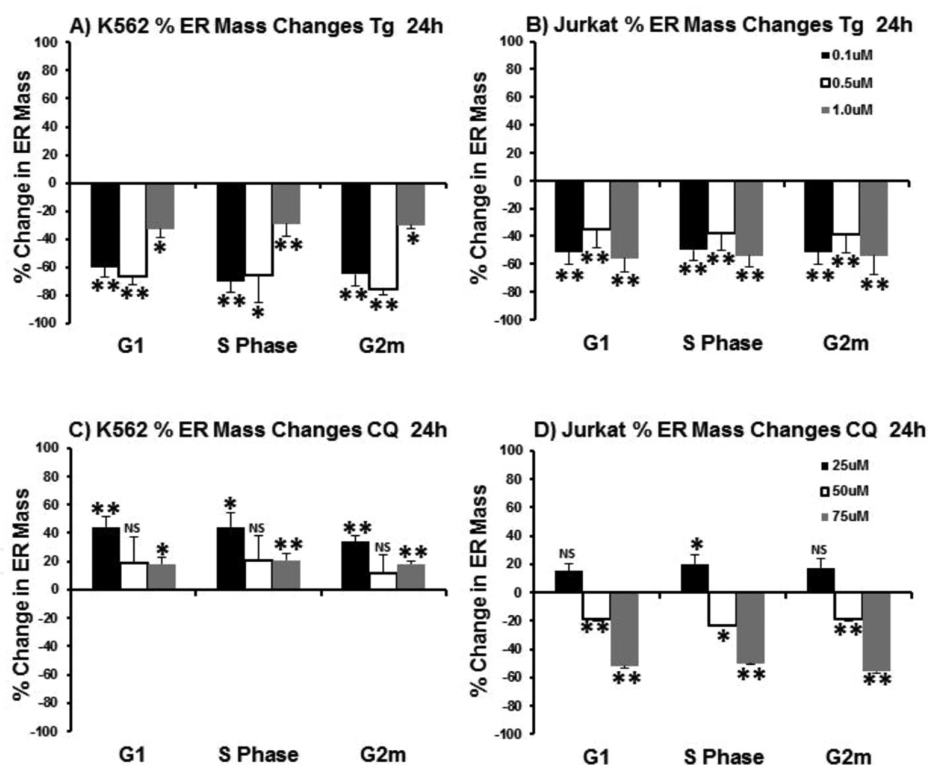

Figure 2. Jurkat and K562 cell lines were untreated or treated with Tg (0.1, 0.5, 1 μM) or CQ (25, 50, 75 μM) for 24 h. Cells were loaded with Hoechst 33342 (15 μg/ml), ERTR (100 nM) and DRAQ7 (2.5 μM) for 1, 0.5 and 0.25 h at 37°C, respectively. Cells were gated as described in Section 2; see **Figure 1**. ERTR test MFI were normalised against the control and a percentage change in the test ERTR signal was calculated. Percentage changes in ER mass of K562 (A) and Jurkat cells (B) treated with Tg were made for G_1, S and G_2m phases of the cell cycle. Percentage changes in ER mass of K562 (C) and Jurkat cells (D) treated with Tg or CQ were made for G_1, S and G_2m phases of the cell cycle. Student t test, *P <0.05; **P < 0.01; NS, not significant; error bars indicate SEM, n = 3.

cells displayed a lower level of non-cell cycle-dependent ER elongation than that observed in K562 cells (<20%, $P < 0.05$, NS, n = 3, **Figure 2D**). However the higher dose CQ induced a reticulophagy (<20–>50%) which was also non-cell cycle dependent ($P < 0.05$, $P < 0.01$, n = 3, **Figure 2D**).

3.2. ER stress responses: protein misfolding

For estimating the overall level of misfolded proteins after ER stress induction, Tg or CQ cells were fixed, permeabilised and labelled with DAPI and the misfolded protein detection reagent, Proteostat [32]. Flow cytometric analysis of the cell cycle and misfolded protein levels was performed on a Becton Dickinson LSRII after UV and blue laser excitation and fluorescence collected at 460 and 610, nm respectively. The gating strategy for the cell cycle analysis of misfolded proteins is shown in **Figure 3**.
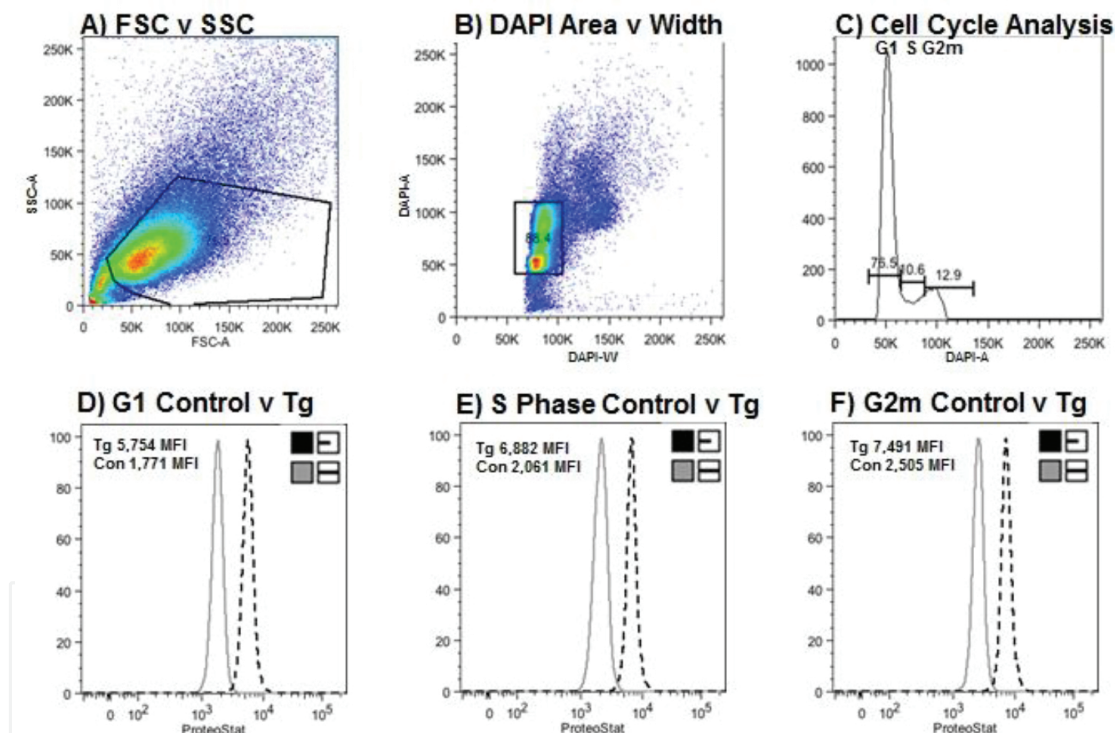

Figure 3. Jurkat and K562 cell lines were untreated or treated with Tg (0.1, 0.5, 1 μM) or CQ (25, 50, 75 μM) for 24 h. Cells were fixed and permeabilised and stained with Proteostat probe (Enzo Life Sciences) according to that described in Section 2. Misfolded protein levels were calculated from the test and untreated Proteostat MFI according to that described in Section 2. The gating strategy employed was to gate on cells through FSC vs. SSC (A) and then gate on single cells using DAPI Area and Width parameters (B). Followed by cell cycle analysis on the DAPI Area parameter, marking off G_1, S and G_2m phases of the cell cycle by virtue that DAPI fluorescence intensity is proportional to DNA content is shown in (C). The Proteostat fluorescence signal is proportional to the level of cellular misfolded proteins, in cells treated with Tg, and was compared to untreated cells in G_1 (D), S (E) and G_2m (F) phases of the cell cycle.

Tg treatment of K562 cells showed a moderately high level of misfolded proteins which were neither dose nor non-cell cycle dependent (>40, $P < 0.05$, $P < 0.01$, n = 3, **Figure 4A**). Jurkat cells

showed a low level of misfolded proteins when treated with Tg which was also not dose nor cell cycle dependent (<35, $P < 0.01$, NS, n = 3, **Figure 4B**). CQ treatment of K562 cells showed a variable level of misfolded proteins which was not cell cycle dependent (25–80, $P < 0.01$, n = 3, **Figure 4C**). In contrast Jurkat cells produced a lower degree of misfolded proteins when treated with CQ (25–40 $P < 0.05$, $P < 0.01$, n = 3)) which was cell cycle dependent in that cells in G_2m had lower amounts of misfolded proteins (**Figure 4D**).
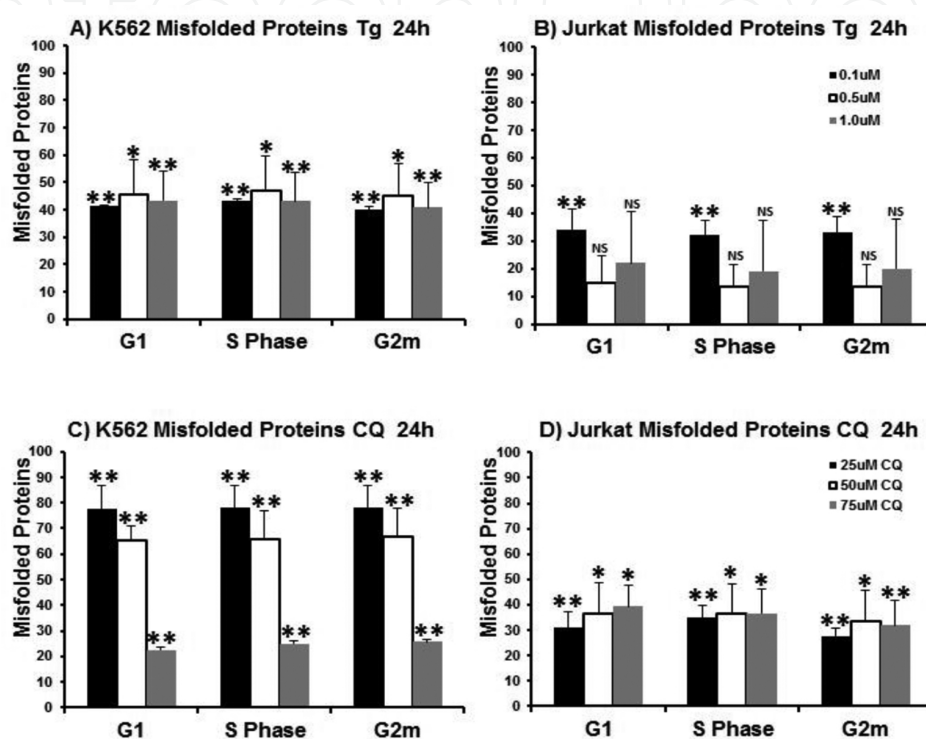

Figure 4. Jurkat and K562 cell lines were untreated or treated with Tg (0.1, 0.5, 1 μM) or CQ (25, 50, 75 μM) for 24 h. Cells were fixed and permeabilised and stained with Proteostat probe (Enzo Life Sciences) according to that described in Section 2; see **Figure 3**. Misfolded protein levels for each phase of the cell cycle (G_1, S and G_2m) were calculated from the test and untreated Proteostat MFI according to that described in Section 2. The level of misfolded proteins in K562 cells is shown in (A) Tg, (C) CQ and Jurkat cells treated with (B) Tg, (D) CQ. Student t test, *$P < 0.05$; **$P < 0.01$; NS, not significant; error bars denote SEM, n = 3.

3.3. ER stress responses: LC3-II-associated autophagy is cell cycle dependent

For estimating the level of autophagy occurring in cells treated with ER stress-inducing drugs, Tg and CQ cells were fixed, permeabilised and labelled with DAPI cells and anti-LC3-II-Alexa Fluor-647 which were collected on a Becton Dickinson LSRII after UV and red laser excitation and fluorescence collected at 460 and 660 nm, respectively. The gating strategy for the cell cycle analysis of LC3-II is shown in **Figure 5**.

Although Tg induced a high degree of ER stress in K562 cells and a lower order in Jurkat cells after 24 h, LC3-II did not increase above control levels (data not shown). However CQ did induce a cell cycle-dependent increase of LC3-II for both cell lines employed in this study

(**Figure 6A** and **B**). Both cell types showed a similar level of LC3-II in that 25 and 75 μM CQ showed a dose and cell cycle-dependent increase above control levels (**Figure 6A** and **B**), whereas 50 μM CQ showed a lower degree of LC3-II upregulation than the other doses of CQ employed in this study (**Figure 6A** and **B**).
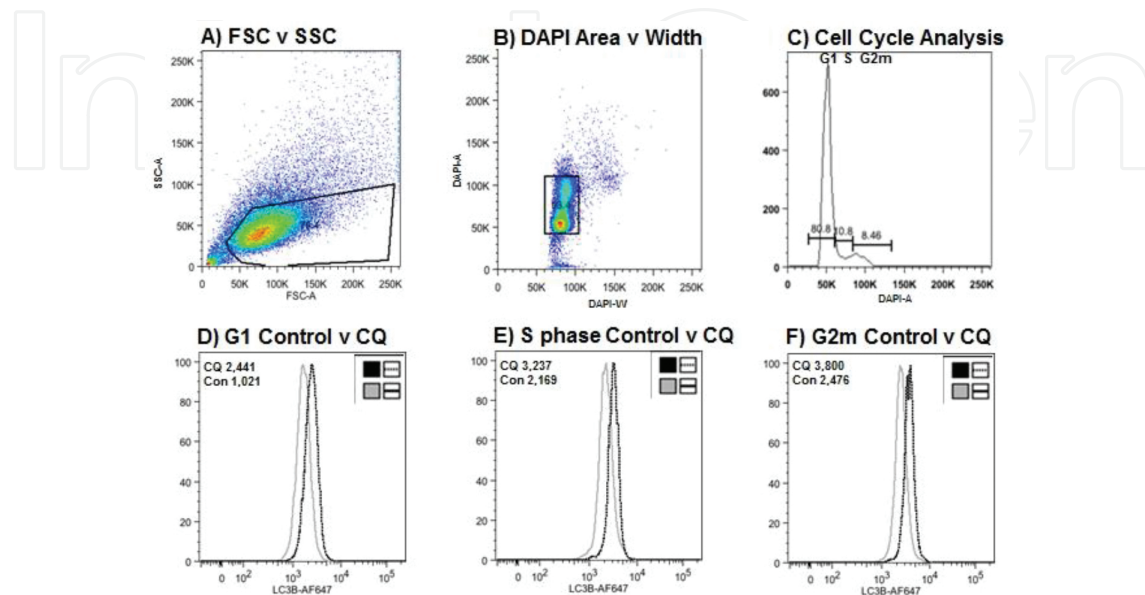

Figure 5. Jurkat and K562 cell lines were untreated or treated with Tg (0.1, 0.5, 1 μM) or CQ (25, 50, 75 μM) for 24 h. Cells were fixed and permeabilised and stained with anti-LC3-II and Alexa Fluor-647 according to that described in Section 2. LC3-II MFI test samples were subtracted from untreated cells according to that described in Section 2. The gating strategy employed was to gate on cells through FSC vs. SSC (A). Single cells were gated using DAPI Area and Width parameters (B). Followed by cell cycle analysis on the DAPI Area parameter, marking off G_1, S and G_2m phases of the cell cycle by virtue that DAPI fluorescence intensity is proportional to DNA content is shown in (C). The LC3-II MFI of CQ treated cells was subtracted from untreated cells in G_1 (D), S (E) and G_2m (F) phases of the cell cycle.
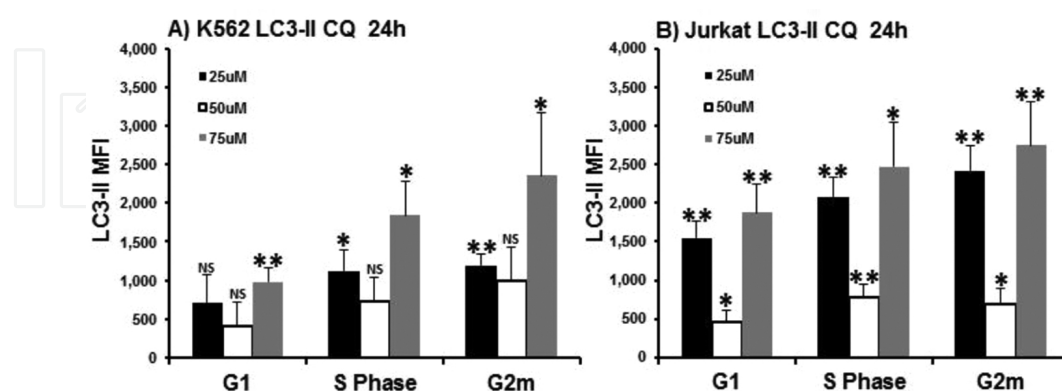

Figure 6. Jurkat and K562 cell lines were untreated or treated with CQ (25, 50, 75 μM) for 24 h. Cells were then fixed, permeabilised and labelled with rabbit anti-LC3-II-AF-647 and DAPI for cell cycle analysis. After gating as described in Section 2 (see **Figure 5**), the LC3-II MFI levels in test samples (test MFI-control MFI) were determined for all cell cycle phases. The levels of LC3-II in K562 (A) and Jurkat cells (B) treated with CQ were calculated for G_1, S and G_2m phases of the cell cycle. Student t test, $*P < 0.05$; $**P < 0.01$; NS, not significant; error bars indicate SEM, n = 3.

4. Discussion

Flow cytometry can be used to investigate ER stress, a biological process not much analysed by this experimental approach to date. Here we measured the end products of ER stress, that is, reticulophagy and misfolded proteins rather second messengers associated with the process, for example, PERK, IRE-1 and ATF6. However the use of live cells and ER Tracker probes to measure reticulophagy has been previously used to estimate the degree of reticulophagy [35, 36], although not in a cell cycle-dependent manner. Analysis of these cells under fixed conditions allowed flow cytometry to estimate the level of misfolded proteins present in the cell (rather than exclusively in the ER) in a cell cycle-dependent manner. The assays employed using just two or three fluorescent probes allowed for a relatively easy flow cytometric analysis, without the need for colour compensation or correction of the bleed through of the different fluorophores into each other, thus avoiding false readings and incorrect conclusions from the acquired data sets. Gating strategies used were as simple as possible, but given the relatively complex nature of the gating needed, they all employed the same approach. This study employed known ER stress-inducing drug Tg, as well as by comparison CQ, and used two cell types to show potential different responses to these drugs. To this end Tg was shown to induce ER stress after 24 h in both cell lines with the ER in such cells undergoing a significant degree of reticulophagy. K562 cells were more affected than Jurkat T cells, whereas only K562 cells showed a reticulophagy, which was more pronounced in specific phases of the cell cycle with the different concentrations of the drug.

The drug CQ, a known initiator of autophagy and apoptosis (although the drug also blocks the process at the lysosome-autophagosome fusion step), was also tested for its ER stress-inducing qualities [12, 32, 33]. CQ appeared to induce ER stress in both cell lines, with Jurkat cells treated with high concentration of CQ displaying a high level of reticulophagy like that observed with Tg. However lower doses of CQ induced ER stress which was typified by an elongation of the ER in Jurkat cells which was again not cell cycle dependent. This mode of action of CQ causing an elongation of the ER was repeated in K562 cells which was cell cycle dependent. Here the degree of elongation reduced as the cell moved through the cell cycle. Thus G_2m cells showed the least amount of ER elongation and hence were more stressed than cells in the G_1 phase of the cell cycle.

Induction of ER stress by both Tg and CQ was further confirmed by the detection of misfolded proteins in a non-cell cycle-dependent manner above that found in untreated cells (except G_2m phase Jurkat cells treated with CQ). K562 cells had a high level of misfolded proteins in response to both Tg and CQ even though Tg induced a reticulophagy and CQ an ER elongation. Similarly Jurkat cells responded to Tg and CQ with a moderate level of misfolded proteins, with most cells displaying a reticulophagy in this instance. Thus, although cells were displaying ER elongation as well as reticulophagy with the different drugs, misfolded proteins were detectable and the highest level found in cells undergoing ER elongation rather than reticulophagy, this perhaps being a reflection that cells with less ER have less space for misfolded proteins and thus a lower level of misfolded proteins.

Although Tg induced a high degree of reticulophagy and misfolded proteins in both cell lines, there was no evidence of autophagy as LC3-II levels did not increase above control levels. However CQ shown previously and in this study to induce ER stress did show an increase LC3-II in a cell cycle-dependent manner in both cell lines.

Thus, the degree and mode of action of these two drugs appear to be cell type dependent, with K562 cells displaying a cell cycle-dependent ER stress response to both drugs, whereas Jurkat cells did not. However, the induction of the autophagic response (the process being blocked at the lysosome fusion step) to CQ was cell cycle dependent in both cell lines. While Tg did not induce an autophagic response in either cell line after 24 h. The type of cell employed and the cell cycle-dependent modulation of these biological processes involved in ER stress and autophagy should be considered when designing studies in ER stress and autophagy. Flow cytometry makes the analysis of these cell cycle-dependent events in the ER stress process easily measureable.

Author details

Ashik Asvin Patel and Gary Warnes[*]

*Address all correspondence to: g.warnes@qmul.ac.uk

Flow Cytometry Core Facility, Blizard Institute, Barts and The London School of Medicine and Dentistry, Queen Mary University London, London, UK

References

[1] Rosello A, Warnes G, Meier U. Cell death pathways and autophagy in the central nervous system and its involvement in neurodegeneration, immunity and CNS infection: to die or not to die—that is the question. Clinical and Experimental Immunology. 2012;168:52–7.

[2] Yang Z, Klionsky D. Eaten alive: a history of macroautophagy. Nature Cell Biology. 2010;12(9):814–22.

[3] Ogata M, Hino S, Saito A, et al. Autophagy is activated for cell survival after endoplasmic reticulum stress. Molecular and Cellular Biology. 2006;26(24):9220–31.

[4] Chen Y, Brandizzi F. IRE1: ER stress sensor and cell fate executor. Trends in Cell Biology. 2013;23(11):547–55.

[5] Moretti L, Cha YI, Niermann KJ, Lu B. Switch between apoptosis and autophagy: radiation-induced endoplasmic reticulum stress? Cell Cycle. 2007;6(7):793–8.

[6] Furuya Y, Lundmo P, Short AD, Gill DL, Isaacs JT. The role of calcium, pH, and cell proliferation in the programmed (apoptotic) death of androgen-independent prostatic cancer cells induced by thapsigargin. Cancer Research. 1994;54:6167–75.

[7] Lin X, Denmeade R, Cisek L, Isaccs J. Mechanism and role of growth arrest in programmed (apoptotic) death of prostatic cancer cells induced by Thapsigargin. The Prostate. 1997;33:201–7.

[8] Ganley I, Wong P, Gammoh N, Jiang X. Distinct autophagosomal–lysosomal fusion mechanism revealed by thapsigargin-induced autophagy arrest. Molecular Cell. 2011;42(6):731–43.

[9] Yorimitsu T, Klionsky DJ. Eating the endoplasmic reticulum: quality control by autophagy. Trends in Cell Biology. 2007;17(6):279–85.

[10] Hoyer-Hansen M, Jaattela M. Connecting endoplasmic reticulum stress to autophagy by unfolded protein response and calcium. Cell Death and Differentiation. 2007;14(9): 1576–82.

[11] Klionsky DJ. Guidelines for the use and interpretation of assays for monitoring autophagy (3rd edition). Autophagy. 2016;12(1):1–222.

[12] Choi JH, Yoon JS, Won YW, Park BB, Lee YY. Chloroquine enhances the chemotherapeutic activity of 5-fluorouracil in a colon cancer cell line via cell cycle alteration. APMIS: Acta Pathologica, Microbiologica, et Immunologica Scandinavica. 2012;120(7): 597–604.

[13] Ashford TP, Porter K. Cytoplasmic components in hepatic cell lysosomes. The Journal of Cell Biology. 1962;12:198–202.

[14] Deter RL, Duve CD. Influence of glucagon, an inducer of cellular autophagy, on some physical properties of rat liver lysosomes. The Journal of Cell Biology. 1967;33:437–49.

[15] Tooze SA, Yoshimori T. The origin of the autophagosomal membrane. Nature Cell Biology. 2010;12(9):831–5.

[16] Mehrpour M, Esclatine A, Beau I, Codogno P. Overview of macroautophagy regulation in mammalian cells. Cell Research. 2010;20(7):748–62.

[17] Ge JN, Huang D, Xiao T, et al. Effect of starvation-induced autophagy on cell cycle of tumor cells. Chinese Journal of Cancer. 2008;27(8):102–8.

[18] Komatsu M, Ichimura Y. MBSJ MCC Young Scientist Award 2009: selective autophagy regulates various cellular functions. Genes to Cells. 2010;15(9):923–33.

[19] Hailey DW, Rambold AS, Satpute-Krishnan P, et al. Mitochondria supply membranes for autophagosome biogenesis during starvation. Cell. 2010;141(4): 656–67.

[20] Kim I, Rodriguezenriquez S, Lemasters J. Selective degradation of mitochondria by mitophagy. Archives of Biochemistry and Biophysics. 2007;462(2):245–53.

[21] Kabeya Y, Mizushima N, Ueno T, et al. LC3, a mammalian homologue of yeast Apg8p, is localized in autophagosome membranes after processing. EMBO. 2000;19(21):5720–8.

[22] Barth S, Glick D, Macleod K. Autophagy: assays and artifacts. The Journal of Pathology. 2010;221(2):117–24.

[23] Hansen TE, Johansen T. Following autophagy step by step. BMC Biology. 2011;9(39):1–4.

[24] Shvets E, Fass E, Elazar Z. Utilizing flow cytometry to monitor autophagy in living mammalian cells. Autophagy. 2008;4(5):621–8.

[25] Kimura S, Noda T, Yoshimori T. Dissection of the autophagosome maturation process by a novel reporter protein, tandem fluorescent-tagged LC3. Autophagy. 2007;3(5):452–60.

[26] Wu YT, Tan HL, Huang Q, et al. Autophagy plays a protective role during zVAD-induced necrotic cell death. Autophagy. 2008;4(4):457–66.

[27] Thomas S, Thurn KT, Biçaku E, Marchion DC, Münster N. Addition of a histone deacetylase inhibitor redirects tamoxifen-treated breast cancer cells into apoptosis, which is opposed by the induction of autophagy. Breast Cancer Research and Treatment. 2011;130(2):437–47.

[28] Geng Y, Kohil L, Klocke BJ, Roth KA. Chloroquine-induced autophagic vacuole accumulation and cell death in glioma cells is p53 independent. Neuro-Oncology. 2010;12(5):473–81.

[29] Chen Y, McMillan-Ward E, Kong J, Israels SJ, Gibson SB. Oxidative stress induces autophagic cell death independent of apoptosis in transformed and cancer cells. Cell Death and Differentiation. 2007;15(1):171–82.

[30] Kaminskyy V, Abdi A, Zhivotovosky B. A quantitative assay for the monitoring of autophagosome accumulation in different phases of the cell cycle. Autophagy. 2011;7(1):83–90.

[31] Warnes G. Flow cytometric assays for the study of autophagy. Methods. 2015;82:21–8.

[32] Shen D, Coleman J, Chan E, et al. Novel cell- and tissue-based assays for detecting misfolded and aggregated protein accumulation within aggresomes and inclusion bodies. Cell Biochemistry and Biophysics. 2011;60(3):173–85.

[33] Chikte S, Panchal N, Warnes G. Use of lysotracker dyes: a flow cytometric study of autophagy. Cytometry A. 2014;85A(2):169–78.

[34] Warnes G. Measurement of autophagy by flow cytometry. Current Protocols in Cytometry. 2014:9.45.1–10.

[35] Panchal N, Chikte S, Wilbourn BR, Meier UC, Warnes G. Autophagy—a double-edged sword—cell survival or death? Flow cytometric measurement of cell organelle autophagy. Intech Open Access Publisher. 2013.

[36] Jia W, Pua HH, Li QJ, He Y. Autophagy regulates endoplasmic reticulum homeostasis and calcium mobilization in T lymphocytes. The Journal of Immunology. 2010;186(3): 1564–74.